



September 2007

Dumbbell Rattling in Thermoelectric Zinc Antimony

W. Schweika

R. P. Hermann

M. Prager

J. Perßon

Veerle Keppens

University of Tennessee, Knoxville, vkeppens@utk.edu

Follow this and additional works at: https://trace.tennessee.edu/utk_matepubs

 Part of the [Materials Science and Engineering Commons](#)

Recommended Citation

Schweika, W.; Hermann, R. P.; Prager, M.; Perßon, J.; and Keppens, Veerle, "Dumbbell Rattling in Thermoelectric Zinc Antimony" (2007). *Faculty Publications and Other Works -- Materials Science & Engineering*.

https://trace.tennessee.edu/utk_matepubs/7

This Article is brought to you for free and open access by the Engineering -- Faculty Publications and Other Works at TRACE: Tennessee Research and Creative Exchange. It has been accepted for inclusion in Faculty Publications and Other Works -- Materials Science & Engineering by an authorized administrator of TRACE: Tennessee Research and Creative Exchange. For more information, please contact trace@utk.edu.



Dumbbell Rattling in Thermoelectric Zinc Antimony

W. Schweika,¹ R. P. Hermann,^{1,2} M. Prager,¹ J. Perßon,¹ and V. Keppens²

¹*Institut für Festkörperforschung, Forschungszentrum Jülich, 52425 Jülich, Germany*

²*Department of Materials Science and Engineering, The University of Tennessee, Knoxville, Tennessee 37996-2200, USA*

(Received 18 April 2007; published 17 September 2007)

Inelastic neutron scattering measurements on thermoelectric Zn_4Sb_3 reveal a dominant soft local phonon mode at 5.3(1) meV. The form factor of this local mode is characteristic for dumbbells vibrating preferably along the dumbbell axis and can be related to a vibration of Sb dimers along the c axis. The Lorentzian width of the mode corresponds to short phonon lifetimes of 0.39(2) ps and yields an estimate of the thermal conductivity that agrees quantitatively with recent steady state measurements. Heat capacity measurements are consistent with an Einstein mode model describing the local Sb-dimer rattling mode with an Einstein temperature of 62(1) K. Our study suggests that soft localized phonon modes in crystalline solids are not restricted to cage-like structures and are likely to be a universal feature of good thermoelectric materials.

DOI: 10.1103/PhysRevLett.99.125501

PACS numbers: 63.20.Pw, 61.12.-q, 65.40.Ba

A significant reduction in energy consumption through the recovery of waste heat could be achieved by efficient materials for thermoelectric power generation [1,2]. Efficient thermoelectric materials require “electron crystal, phonon glass” behavior, combining both good electric and poor thermal conductivity [3]. Both parameters, σ and κ respectively, determine the figure of merit $ZT = S^2\sigma T/(\kappa_e + \kappa_l)$ of a thermoelectric material, where T , S , κ_e , and κ_l are the temperature, Seebeck coefficient, and electronic and lattice contribution to the thermal conductivity, respectively. Good thermoelectric materials with $ZT > 1$ are typically semiconductors, in which doping maximizes $S^2\sigma$, while crystalline order preserves high carrier mobility. The lattice thermal conductivity κ_l plays a key role in optimizing the figure of merit, since κ_e is proportional to σ (Wiedemann-Franz law). Traditional concepts of phonon scattering are based on structural disorder and consider point defects with either atomic substitution altering mass and bond stiffness, or filling of cage-like structures such as the skutterudites [4–6] and clathrates [7,8] by heavy incoherently rattling atoms, and more recently, larger defects in nanostructured materials [9].

Among thermoelectric materials, zinc antimony, known in literature as Zn_4Sb_3 , exhibits an outstanding figure of merit between 450 K and 670 K with $ZT = 1.3$ at 670 K, owing to its particularly low thermal conductivity [10,11]. Sufficient electronic conductivity follows from a low electronic carrier concentration accompanied by high carrier mobility in this rather covalent material [12]. The structure and precise stoichiometry of Zn_4Sb_3 has been under debate for decades [13–18]. The proposed structures are variants of the Zn_6Sb_5 unit cell, shown in Fig. 1, including structural disorder due to additional Zn interstitials ($\approx 17\%$) and Zn vacancies ($\approx 10\%$) [13,14,18] and have been derived from comprehensive diffraction studies and analyses by maximum entropy methods. The conjecture has been made that the structural Zn disorder associated with interstitials

and vacancies causes phonon scattering and explains the low thermal conductivity [13,14]. However, efficient phonon scattering can be expected from the interaction of the heat carrying acoustic phonons with phonons that are sufficiently low in energy to cross the acoustic branches and are highly thermally populated, directing research towards soft local modes. In view of masses and bonding distances in Zn_4Sb_3 , rather than the Zn interstitials, a more likely candidate for such a soft mode is the rattling of the heavy Sb_2 dumbbells (12c site; see Fig. 1), particularly so because the dimerization of antimony along the c axis into tightly bonded dumbbells opens rattling space.

Herein we report inelastic neutron scattering and heat capacity measurements that identify in Zn_4Sb_3 a new type of dynamical disorder: soft localized dumbbell vibrations of Sb dimers with an energy of 5.3 meV (62 K). This dynamic disorder evolves from regular atoms rather than from structural disorder and is believed to be the origin of low thermal conductivity found in this material.

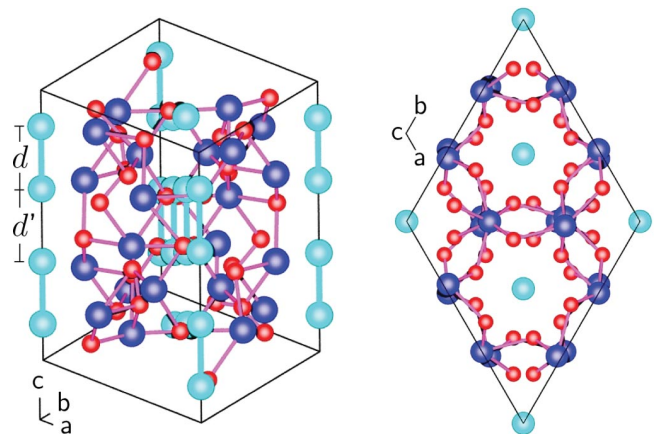


FIG. 1 (color). The idealized crystal structure of the Zn_4Sb_3 site forms dimers, i.e., $d < d'$, oriented along the c axis in channels of distorted hexagonal layers of Sb and Zn, on the 18e and 36f sites, respectively.

The sample has been prepared by direct reaction of the constituent elements from an ingot with the nominal composition of Zn_4Sb_3 . Zn, purity >0.99999 , etched to remove oxides, and Sb, purity >0.999 , have been molten in sealed quartz tube under 800 mbar Ar atmosphere. The phase purity of the sample has been checked by x-ray powder diffraction and the pattern agrees with Ref. [13]. The heat capacity measurement was performed on 9.2 mg of Zn_4Sb_3 between 2 and 300 K in a physical property measurement system from Quantum Design. The measured heat capacity is identical to that reported in Ref. [10], except for a sharper signature of the first order phase transition at ~ 250 K in the present sample.

Our heat capacity measurements of Zn_4Sb_3 reveal the signature of a prominent soft local mode in the low temperature regime; see Fig. 2. Within a simple model, one Einstein mode in addition to the Debye contribution is required to account for the heat capacity. This modeling yields that 15% of the atomic degrees of freedom exhibit an Einstein oscillator behavior with energy $E_r = 5.3(1)$ meV, and a Debye temperature of 240(2) K for the remaining average phonon contribution. The heat capacity also exhibits the structural transition[17] observed near 255 K. A possible explanation for the Einstein mode can be given by the rattling of Sb dimers. The high temperature limit of the lattice contribution to heat capacity is $3k_B$ per atom and partial contributions reflect percentages in atomic degrees of freedom. The total atomic fraction of dimerizing Sb atoms is between 17.6% and 19.5% depending on the structural model [13,16]. Assuming that apart from the dimer stretching mode all other 5 out of 6 degrees of freedom of the two dumbbell atoms are involved, they would account for 14.7% to 16.3% of the heat capacity. The opening of rattling space by Sb dimerization occurs in a preferential direction along c , and rattling in a single

direction would only account for 1/6 of the dumbbell degrees of freedom. This constitutes a more likely scenario when including an additional contribution from the drag of neighboring atoms and dumbbell librations at slightly higher energy.

The inelastic neutron scattering experiments have been carried out on the thermal time-of-flight spectrometer SV29 at the Jülich research reactor using a polycrystalline rod of approximately 8 cm^3 Zn_4Sb_3 . The measured background has been subtracted from the data and a standard vanadium calibration has been applied. Inelastic neutron powder scattering may provide an estimate for the phonon density of states and reveal specific correlations in the dynamics. The main feature of the dynamic response in Zn_4Sb_3 observed by neutron scattering (Fig. 3) is a non-dispersive inelastic signal near 5 meV that is symmetric in energy to both sides of the elastic line. The lack of dispersion attests of the localized character of the mode as expected for an Einstein oscillator [19]. The mode must be strongly anharmonic because of its unusual intrinsic width. Most importantly, the inelastic coherent scattering intensity does not increase monotonically with scattering angle as would be expected for phonon scattering of individual atoms, but instead the intensity modulation is characteristic of the pair correlation of a dimer.

The neutron scattering amplitudes of Zn and Sb are similar and their scattering is essentially coherent. For powder scattering, with orientational averaging, the average phonon intensity ($\propto Q^2$) is modulated by the characteristic pair correlation of the Sb dumbbell, i.e., a Bessel function $\sin x/x$, where $x = Qd$, $Q = 4\pi \sin\theta/\lambda$ is the modulus of the scattering vector, and d is the Sb distance in the dumbbell. The scattering is given by $S(Q, E) \propto \frac{2}{3}x^2[1 + \sin(x)/x]$. In case of preferred directions of the vibrations, an orientational average of the displacement vectors involves higher order Bessel functions; for longitudinal modes (vibrations along the dumbbell axis) we obtain $S(Q, E) \propto \frac{2}{3}x^2[1 + 3\sin(x)/x + 6\cos(x)/x^2 - 6\sin(x)/x^3]$.

For a quantitative analysis we consider three models for the soft vibrations of dumbbells: (i) isotropic modes, (ii) longitudinal modes along the dumbbell axis, and (iii) weakly coupled longitudinal dumbbell modes; see Fig. 3. Assuming a damped harmonic oscillator, the energy dependence is described by a Lorentzian. Further data analysis shows an additional broad component, centered at $E = 0$, essentially related to multiphonon processes. This contribution is modeled by a Gaussian with intensity proportional to the square of the scattering vector Q , Q -independent width, and centered at zero energy transfer. The parameters of the model refinements are shown in Table I. All considered models provide close quantitative descriptions of the observed inelastic scattering. The pronounced Q dependence of the measured inelastic scattering is well reproduced by dimer oscillations along the dimer

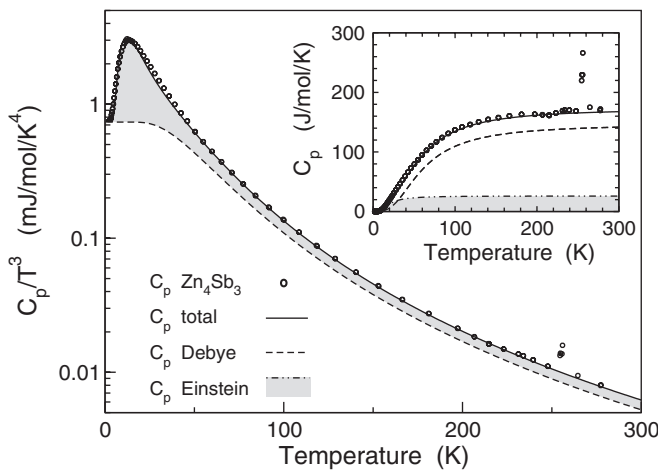


FIG. 2. The heat capacity of Zn_4Sb_3 . The sum of a Debye contribution with a Debye temperature of 240 K and a soft 62 K or 5.3 meV Einstein mode accurately describes the measured heat capacity.

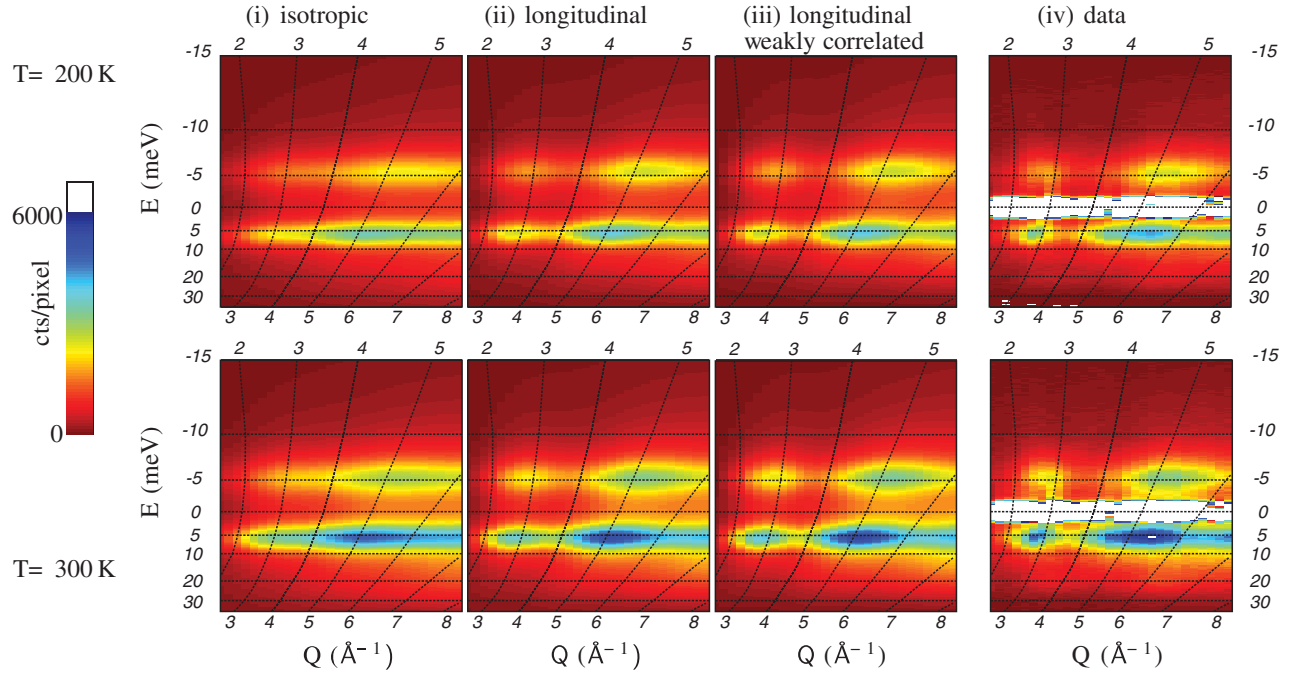


FIG. 3 (color). Inelastic neutron time-of-flight data (iv) compared to calculations with a damped harmonic oscillator (Lorentzian) with a dumbbell form factor, and multiphonon contribution (Gaussian) at 200 and 300 K: (i) an isotropic dumbbell mode, (ii) a longitudinal dumbbell mode, (iii) a weakly correlated longitudinal dumbbell mode.

axis, model (ii) or (iii). Possible correlations to neighboring dumbbells are considered in model (iii); a weak negative correlation between the dumbbells of about 6% indicates that dumbbells are almost independent but seem to be oscillating antiphase. This model of weakly coupled, longitudinal dumbbells best reproduces the observed inelastic scattering.

The observed distance, $d = 2.75 \text{ \AA}$ is typical for near neighbor distances in this material though it is slightly smaller than the 2.82 \AA expected for the Sb dimers according to previous structural x-ray studies [13,15,16]. The difference may arise from the different types of observa-

tion: inelastic neutron scattering yields the true distance between the two swinging Sb nuclei, whereas (the energy integrated) x-ray diffraction yields the average electron density distribution, that, in the case of anharmonic oscillations, will be smeared out towards a slightly larger dumbbell distance. The observed strongly anharmonic rattling of the dumbbell is indicative of a rather shallow potential and in agreement with the unusually large fraction of multiphonon scattering and the large mean square displacements. For longitudinal dumbbell modes, $2W/Q^2$ corresponds to a mean square displacement $u_{33}^2 \approx 0.04 \text{ \AA}^2$ along the dumbbell axis only, indicative of a tubelike

TABLE I. Energy E_r and Lorentzian width (HWHM) Γ_r of the dimer mode for isotropic displacements, longitudinal displacements (LD) along the dimer axis, and including correlations to next dimers. α is the dumbbell correlation in model (iii). A_L and A_G are proportional to the amplitudes of Lorentzian and Gaussian, modeling the dumbbell oscillation and multiphonon contribution, respectively. Mean square displacement parameters of the dumbbell can be derived from the Debye-Waller factor e^{-2W} , and w_G is the FWHM of the Gaussian. Residuals are given by $R = \sum (I_{\text{obs}} - I_{\text{th}})^2 / \sum I_{\text{obs}}^2$, where I_{obs} and I_{th} are the observed and calculated intensities, respectively. Standard statistical deviations are given in parentheses.

Dimer model	E_r (meV)	Γ_r (meV)	A_L	d (\AA)	$2W/Q^2$ (\AA^2)	w_G (meV)	A_G	R (%)
300 K								
(i) isotropic	5.22(3)	1.95(10)	0.121(15)	2.77(3)	0.041(6)	18.1(2.0)	0.028(3)	4.1
(ii) LD	5.23(2)	1.81(5)	0.114(15)	2.75(2)	0.042(3)	16.0(1.5)	0.031(2)	2.3
(iii) LD, $\alpha = -0.06$	5.23(2)	1.69(5)	0.144(15)	2.75(2)	0.043(3)	14.1(1.5)	0.034(2)	2.0
200 K								
(i) isotropic	5.37(3)	1.80(10)	0.080(15)	2.78(3)	0.037(6)	19.8(2.0)	0.020(3)	4.2
(ii) LD	5.36(2)	1.68(7)	0.094(15)	2.75(2)	0.039(4)	16.6(1.5)	0.021(2)	2.9
(iii) LD, $\alpha = -0.066$	5.38(2)	1.65(7)	0.098(15)	2.75(2)	0.040(4)	14.4(1.5)	0.026(2)	3.0

confinement of the dumbbells. Considering neighboring Sb dimers, their longitudinal displacements are limited to 2 times the (FWHM) displacements, $2\sigma = 2\sqrt{(2u_{33}^2/\ln 2)} = 0.7 \text{ \AA}$. In view of the four Sb distances and a dimerization with $d = 2.75 \text{ \AA}$ within the $c = 12.4 \text{ \AA}$ unit cell spacing, this large displacement means a full occupation of the rattling space, where $d' \approx d + 2\sigma$; see Fig. 1. Inelastic neutron scattering selectively yields the atomic displacement parameter (ADP) of this specific local mode. The Debye-Waller factor, interpreted essentially in terms of u_{33}^2 of Sb on the $12c$ site, is also in quantitative agreement with ADPs from structure refinements, when taking into account that these are isotropic ADPs.

The excitation energies are in perfect agreement with the specific heat measurements, which also indicate a dominant local Einstein mode of 5.3 meV. The phonon damping related to the Lorentzian width results from interactions between local dimer phonon modes and the propagating acoustic phonon modes and corresponds to their very short phonon lifetime, $\tau = \hbar/\Gamma \approx 3.9 \times 10^{-13} \text{ s}$ at 300 K. With a mean sound velocity of $v_s = 2.47 \times 10^5 \text{ cm s}^{-1}$ (Ref. [10]), this lifetime yields the mean free path of the heat carrying acoustic phonons, $l \approx 0.96 \text{ nm}$, and is similar to unit cell dimensions. Assuming that these phonon interactions are the dominant scattering term for the heat transport, a simple kinetic gas theory model yields a thermal conductivity $\kappa = c_v v_s l/3 \approx 13.2 \text{ mW K}^{-1} \text{ cm}^{-1}$, where $c_v = 1.68 \text{ J K}^{-1} \text{ cm}^{-3}$ is the specific heat (per unit volume) at 300 K, close to the Dulong-Petit limit. This estimation agrees favorably with the recently measured lattice thermal conductivity $\kappa \approx 13 \text{ mW K}^{-1} \text{ cm}^{-1}$ at 300 K obtained by the steady state method [10]. These results are at variance with an earlier lower estimation [11], obtained by thermal diffusivity, involving a smaller heat capacity, smaller sound velocity and a larger carrier concentration. No abrupt change is seen in the thermal conductivity [10] near 255 K at the order-disorder transition involving Zn atoms [17]. Such a change would be expected if Zn disorder were playing a dominant role in the observed local mode. On the other hand, the dumbbell modes are, as we found by the measurements at 200 and 300 K, not affected by the transition. The inelastic intensities scale fairly well with temperature: therefore, the phonon density of states is essentially temperature independent.

In conclusion, inelastic neutron scattering reveals local soft and strongly anharmonic modes of Sb dimers that dominate and drive the dynamic response. The dynamic disorder by soft dumbbell modes of antimony is quantitatively consistent with the low thermal conductivity in zinc antimony. The present result underscores that dynamic “rattling” disorder is crucial for thermoelectric properties and is a feature not restricted to single atoms in cage structures. Here, the size of the objects scattering the phonons is intermediate between single rattling atoms and nanosized objects in superlattice structures [9] whose

phonon scattering mechanisms are yet to be explored. Vibrating Sb dumbbells are a striking illustration of “*schwingende Elementargebilde*”, the general term originally used in Einstein’s centennial work [20]. The search for structures with such more complex *swinging elementary units* and exploiting their anisotropic properties may pave new ways for thermoelectric material research.

We gratefully acknowledge comments and discussions with P. Dederichs, M. Monkenbusch, and D. Mandrus. Work at The University of Tennessee is supported by the National Science Foundation under Grant No. DMR 0506292.

-
- [1] J. Yang and Th. Caillat, *Mater. Res. Bull.* **31**, 224 (2006).
 - [2] G. A. Slack, in *CRC Handbook of Thermoelectrics*, edited by D. M. Rowe (CRC, Boca Raton, 1995), p. 407.
 - [3] V. Keppens, D. Mandrus, B. C. Sales, B. C. Chakoumakos, P. Dai, R. Coldea, M. B. Maple, D. A. Gajewski, E. J. Freeman, and S. Bennington, *Nature (London)* **395**, 876 (1998).
 - [4] B. C. Sales, D. Mandrus, and R. K. Williams, *Science* **272**, 1325 (1996).
 - [5] R. P. Hermann, R. Jin, W. Schweika, F. Grandjean, D. Mandrus, B. C. Sales, and G. J. Long, *Phys. Rev. Lett.* **90**, 135505 (2003).
 - [6] B. C. Sales, B. C. Chakoumakos, and D. Mandrus, *Phys. Rev. B* **61**, 2475 (2000).
 - [7] R. P. Hermann, W. Schweika, O. Leupold, R. Rüffer, G. S. Nolas, F. Grandjean, and G. J. Long, *Phys. Rev. B* **72**, 174301 (2005).
 - [8] M. Christensen, F. Juranyi, and B. B. Iversen, *Physica (Amsterdam)* **385–386B**, 505 (2006).
 - [9] W. Kim, J. Zide, A. Gossard, D. Klenov, S. Stemmer, A. Shakouri, and A. Majumdar, *Phys. Rev. Lett.* **96**, 045901 (2006).
 - [10] S. Bhattacharya, R. P. Hermann, V. Keppens, T. M. Tritt, and G. J. Snyder, *Phys. Rev. B* **74**, 134108 (2006).
 - [11] Th. Caillat, J.-P. Fleurial, and A. Borshevsky, *J. Phys. Chem. Solids* **58**, 1119 (1997).
 - [12] S.-G. Kim, I. I. Mazin, and D. J. Singh, *Phys. Rev. B* **57**, 6199 (1998).
 - [13] G. J. Snyder, M. Christensen, E. Nishibori, and T. Caillat, *Nat. Mater.* **3**, 458 (2004).
 - [14] F. Cargnoni, E. Nishibori, Ph. Rabiller, L. Bertini, G. J. Snyder, M. Christensen, C. Gatti, and B. B. Iversen, *Chem. Eur. J.* **10**, 3861 (2004).
 - [15] H. W. Mayer, I. Mikhail, and K. Schubert, *J. Less Common Met.* **59**, 43 (1978).
 - [16] Y. Mozharivsky, A. O. Pecharsky, S. Bud’ko, and G. Miller, *Chem. Mater.* **16**, 1580 (2004).
 - [17] J. Nylen, M. Andersson, S. Lidin, and U. Häussermann, *J. Am. Chem. Soc.* **126**, 16306 (2004).
 - [18] Y. Mozharivsky, Y. Janssen, J. L. Harringa, A. Kracher, A. O. Tsokol, and G. J. Miller, *Chem. Mater.* **18**, 822 (2006).
 - [19] R. P. Hermann, F. Grandjean, and G. J. Long, *Am. J. Phys.* **73**, 110 (2005).
 - [20] A. Einstein, *Ann. Phys. (Leipzig)* **22**, 180 (1907).